PARTICLE MANIPULATION USING LIGHT'S LINEAR AND ORBITAL-ANGULAR MOMENTUM

by

Sean Cruikshank

A Thesis Submitted to the Faculty of
the Wilkes Honors College
in Partial Fulfillment of the Requirements for the Degree of
Bachelor of Arts in Liberal Arts and Sciences
with a Concentration in Physics

Wilkes Honors College of
Florida Atlantic University
Jupiter, Florida

April 2015

PARTICLE MANIPULATION USING
LIGHT'S LINEAR AND ORBITAL-ANGULAR MOMENTUM

by

Sean Cruikshank

This thesis was prepared under the direction of the candidate's thesis advisor, Dr. Andrew Johnson, and has been approved by the members of his supervisory committee. It was submitted to the faculty of The Honors College and was accepted in partial fulfillment of the requirements for the degree of Bachelor of Arts in Liberal Arts and Sciences.

SUPERVISORY COMMITTEE:

_____

Dr. Andrew Johnson

_____

Dr. Meredith Blue

_____

Dean Jeffrey Buller, Wilkes Honors College

_____

Date

This thesis is based on an experiment done under the supervision of Dr. Warner Miller and Dr. Grigory Kreymerman of Florida Atlantic University's Physics department. Assistance was also provided by Ms. Elizabeth Rubino, an undergraduate physics student of Florida Atlantic University's Charles E. Schmidt College of Science.

Funding for this experiment was provided by generous grants from FAU's Office of Undergraduate Research and Inquiry.

ABSTRACT

Author:	Sean Cruikshank
Title:	Particle Manipulation Using Light's Linear and Orbital-Angular Momentum
Institution:	Wilkes Honors College of Florida Atlantic University
Thesis Advisor:	Dr. Andrew Johnson
Degree:	Bachelor Of Arts in Liberal Arts and Sciences
Concentration:	Physics
Year:	2015

Quantum optics is a subsect of quantum mechanics focused on exploring the properties of light due to its dual nature as both a particle and a wave. One such property that has been of particular interest recently is that of light's momentum, specifically its linear and orbital-angular momentum (OAM). Light carrying both types of momentum are of particular interest to the life sciences due to the linear momentum of light's ability to directly manipulate particles and orbital-angular momentum's potential to unravel DNA spirals. Light carrying orbital-angular momentum has also shown promise in information technology as a new means of sending large amounts of data over long distances. This thesis will provide background on the quantum optics of particle manipulation and the results from experimental studies performed on this topic. The results show evidence of light with both types of momentum being created and used to manipulate particles to different degrees.

To Mom and Dad

Contents

List of Figures

List of Tables

Chapter 1

Introduction

1.1 Modern Optical Theory

The modern understanding of light and optics originated in the early twentieth century. In 1901, while studying the radiation emitted from a black body, Max Planck realized that the energy emitted from a black body could be properly explained if the energy was quantized. Expanding on this, in 1905, Albert Einstein theorized that the energy of all radiation could be quantized to individual points in space. These light quanta not only carried energy but also momentum. Since momentum is a property of particles, this was the birth of the idea of the particle of light, now known as the photon [1].

Einstein's particle nature of light would later be experimentally verified by Arthur Compton [1]. In his experiment, he shot a beam of light through a sample of carbon and noticed upon exiting the light had a longer wavelength. He concluded that this was possible because the light consisted of particles that were losing momentum to the object and therefore had lower energy and longer wavelength [2]. With this experiment, the photon was experimentally verified, leading to the dual particle/wave nature of light.

1.2 Light's Momentum

With the verification that light could indeed be classified as a particle, much more attention was given to the momentum light carried. Traditionally, while theory stated light could have three types of momentum, only two of these types were actually observable. The first of these was spin angular momentum. This type of momentum is associated with the spin value that every particle has. The spin value of light is derived from its circular polarization and can come in one of two values. The angular momentum contribution from spin is $\hbar \times \sigma$ where $\hbar$ is the reduced Planck's constant and σ is an integer value that depends on how the light is polarized: $\sigma = 1$ for left-handed circular polarization and $\sigma = -1$ for right handed circular polarization [3].

The second traditional momentum was linear momentum associated with the particle's propagation through space. For massive particles, this momentum is found through the equation $p = mv$ where m is the mass of the particle and v is its velocity. Photons, however, are massless particles and move at a constant speed (c) known as the speed of light. As such a new momentum relation had to be formulated. The momentum of light was found by Einstein to be related to its wavelength through the relation $p = h/\lambda$ where h is Planck's constant and λ is the wavelength of the light [4]. Beams of light carrying this momentum have a distribution given by the equation

$$E(r,z) = \frac{w_0}{w} \cdot exp\left(\frac{-r^2}{w^2} - ikz - \frac{i\pi r^2}{\lambda R} + i\phi_0\right) \tag{1.1}$$

The terms in this equation are as follows: w_0 is the beam waist radius, w is the beam radius and has a value of $w = w_0[1 + (\frac{\lambda z}{\pi w_0^2})^2]^{1/2}$, r is the perpendicular distance from the axis of propagation, i is the imaginary number, k is the wave

number with value $k = \frac{2\pi}{\lambda}$, λ is the wavelength, R is the radius of curvature, and ϕ_0 is the Gaussian beam phase shift.

Equation 1.1 is a solution to the differential equation

$$\frac{\partial^2\psi}{\partial r^2} + \frac{1}{r}\frac{\partial\psi}{\partial r} - 2ik\frac{\partial\psi}{\partial r} = 0 \tag{1.2}$$

known as the axially symmetric paraxial wave equation in cylindrical coordinates. The derivation of equation 1.1 is well known and is introduced in most entry level optics classes. As such, the full derivation is omitted. To see the full derivation of this equation, please see [7]. Equation 1.1 is known as the Gaussian beam equation and beams of light that are characterized by it are known as Gaussian beams. Most standard laser beams are Gaussian beams.

A third type of momentum associated with light was finally observed in 1992. A group of scientists discovered that if a beam of light was phase shifted to have a certain phase dependence, it would carry orbital angular momentum (OAM). Light beams carrying this type of momentum have an azimuthal phase dependency of $e^{-i\ell\phi}$ where ℓ is the OAM quantum number and can take any positive or negative integer value, and ϕ is an angle and the azimuthal coordinate in the beams cross section [3]. The characteristic equation for beams carrying this type of momentum is

$$E(r,\phi,z) = \left[\frac{2p!}{\pi(p+m)!}\right]^{1/2}\frac{1}{w(z)}\left[\frac{\sqrt{2}r}{w(z)}\right]^m L_{pm}\left(\frac{2r^2}{w^2(z)}\right)\cdot \\ exp\left[\frac{-r^2}{w^2(z)} - ikz - \frac{i\pi r^2}{\lambda R(z)} - i\left(2p+m+1\right)\phi_0(z)\right]\cdot exp\left(im\varphi\right) \tag{1.3}$$

where p and m are the indices of the Laguerre polynomials. This is another,

albeit higher order, solution to the paraxial wave equation in cylindrical coordinates. Again, for the full derivation refer to [7]. This equation is known as the Laguerre-Gaussian beam equation as it carries in it the Laguerre polynomials as well as all of the characteristics of the standard Gaussian beam. To create a Laguerre-Gaussian beam, one must start with a standard Gaussian beam and phase shift it.

1.3 Using Light's Momentum

The importance of light's momentum has been demonstrated its involvement in many recent experiments. In 1970, a group of researchers led by Arthur Ashkin used light to trap a dielectric particle, leading to the creation of what is now referred to as optical tweezers [8]. Researchers in the life sciences would later apply optical tweezers with linear momentum to use trapping and experimenting on cells. One such example of this was an experiment done by Zhang and Liu who were able to trap and manipulate biological cells in ways such as stretching and organizing them [9]. In another experiment [10], optical tweezers using OAM photons have been shown to have the capacity to impart a torque on DNA strands, allowing "the study of DNA transcription under torsion".

Photons carrying OAM also have a potential use in information technology. Data transmission with light involves sending different streams of data over distinct basis states so that the data will not be corrupted. While light beams traditionally could only be created with two angular momentum basis states, corresponding to the two values of spin, the addition of OAM has the potential to add an infinite amount of states corresponding to the fact the quantum number ℓ can take any positive or negative integer value. Indeed, an experiment done by Bzinovic *et. al* showed that this was the case by using OAM states and achieving data transfer rates as high as 400 gigabits-per-second [11].

Due to the importance of both light's linear and orbital-angular momentum, the goal of the experiment on which this thesis was based was to create separate beams carrying both types of momentum and then use those beams to manipulate particles. In order to explain fully the experiment, this thesis will start by explaining the theory behind the major pieces of equipment used. This will be followed by a detailed explanation of the set-up and processes used to create the experiment. The results from the experiment will then be presented and analyzed with the final conclusions to follow.

Chapter 2

Experimental Equipment

In order to achieve the phase change necessary for creating a Laguerre-Gaussian beam mode as well as trapping and observing particles, two pieces of high tech equipment were needed: a spatial light modulator (SLM) and optical tweezers.

2.1 Spatial Light Modulators

A beam of photons does not just come out of a laser with the required azimuthal phase dependence needed for it to carry orbital angular momentum. The beam must first be passed through a diffraction grating or hologram to change its phase dependency. These holograms are generated by "recording [...] the interference pattern made between a plane wave and the beam that one seeks to produce" [4] which, in this situation, is the Laguerre-Gaussian beam. This interference pattern looks like a normal diffraction grating, except for the middle part where a fork appears. This fork changes depending on the value of the quantum number ℓ.

As the equations for both plane waves and Laguerre-Gaussian beams are already known, a computer can easily take the two equations and find the interference between them, producing the needed hologram. This is a code that has been written in many ways across a variety of different programming languages.

For this thesis, two Matlab codes were found and tested to produce the required holograms. The full codes can be found in Appendix C of this thesis [5][6].

The problem arises, however, in getting the beam to pass through the hologram. From the computer, the hologram must be printed onto some medium transparent to light. The medium must also not cut the intensity of the beam by much so as to preserve the beam's capability to influence matter. Because of this, in the past, plastic and glass were used as mediums due to the fact that they had the desired qualities. Holograms were directly printed onto slides of these materials which were then added to experimental setups just like a diffraction grating.

Producing beams with such holograms, however, was highly inefficient in actual experiments due to the myriad amount of parameters that needed to be controlled. Such parameters include every aspect of the hologram itself including what quantum number ℓ is being produced, how far apart the black and white fringes are, and how thick the black lines are compared to the white lines. Each of these parameters can have a great effect on the beam produced and changing them is important to achieving the optimal beam required for the experiment. With printing on glass and plastic, however, changing these parameters was not feasible. This is because if one wanted to change these parameters, one must print out a whole new set of slides, which would require a significant amount of excess time and money.

Spatial Light Modulators are the answer to the limitations of old methods of producing holograms. An SLM is a small electronic device that connects to a computer through a VGA cable. On the SLM itself there is a small LCD in front of a mirror. When connected to a computer, the SLM acts as a second monitor, displaying on the LCD screen whatever is displayed on the computer. The SLM interprets anything white as blank space and takes whatever is displayed in solid

colors on the computer and puts the image on its own LCD. This eliminates the need to make many different slides as all one has to do is produce a new image on the laptop and the SLM will change its LCD accordingly.

Once the hologram is displayed on the SLM, the laser beam simply needs to be aligned with the square LCD. The beam will then be reflected off the mirror behind the LCD and pass through the hologram where it will be phase shifted to a Laguerre-Gaussian beam. If the beam produced does not exactly match what was expected, the hologram on the computer can be moved around, shrunk, or expanded until a perfect beam is achieved. As Miles Padgett puts it, "These devices (SLMs) produce reconfigurable, computer-controlled holograms that allow a simple laser beam to be converted into an exotic beam with almost any desired phase and amplitude structure." [4, 36]

2.2 Optical Tweezers

In order to trap and observe the particles optical tweezers are employed. Optical tweezers utilize a modified high powered microscope and a laser. The laser is shot through an aperture on the side where it will be redirected by a series of mirrors down the path of sight to the tray where the sample is arranged.

Once the beam is set up correctly and is passing through the prepared sample, there are two different ways in which the beam can trap the particles, depending on the size of the particle itself. For particles with dimensions larger than the wavelength, the mechanics behind optical tweezers can be explained fully using ray optics [12]. For particles with dimensions smaller than the laser's wavelength, the force of the trap can only be understood "in terms of the electric field near the trapped particle" [12]. As the only particles used in this experiment were larger than the wavelength of light used (micrometer sized particles versus a nanometer beam), the ray optics approach is sufficient for the present work.

To see how ray optics traps a particle, imagine first that a particle is within the radius of the beam but is displaced a certain distance Δx to the left from the center of the beam. If the center of the beam is where the intensity is the strongest, as it should be for a Gaussian beam, at this position rays of light entering the particle are more intense to the right than they are to the left. As these light rays enter the particle, they are refracted out in a direction towards the center of the particle in the x direction. This means that if a ray enters on the left side of the particle, it will be bent slightly to the right upon exiting and vice versa for a particle entering on the right side.

As light can also be thought of as a particle, this change in direction is equivalent to a change in momentum. Since a change in momentum over time is equal to a force through the equation $\vec{F} = \Delta\vec{p}/\Delta t$, the photon exerts a reactive force on the particle opposite to the direction of its change in momentum. Looking at individual rays again, if the light entered on the left side and is bent right, it would exert a force on the particle to the left. Likewise, a ray of light entering on the right would exert a force to the right.

Going back to the original displaced particle example, adding up the forces of all the rays entering the particle would result in a net force pushing the particle to the left. This is because when displaced to the left, the less intense rays entering the particle on the left carrying smaller momentum would produce a lesser force than the more intense rays on the right carrying greater momentum. The forces from the right rays completely dominate the forces from the left rays, causing the particle to move to the right. Once the particle reached the center, however, it would stop moving completely as it is at this point that the intensity of the rays entering the left side would be completely equal to the intensity entering the right side. It is at this point that the particle is trapped in the lateral direction. For tweezers using beams with OAM, the explanation is similar, but the center of the

beam trap is moving around in a circle of constant radius. The trapped particle, therefore, follows the trap and starts to move in a similar circle.

Chapter 3

Experimental Set-Up

To achieve all the goals set for this project, it was necessary to split the experiment into three stages, each with its own material set-up and end goal. The first phase was dedicated to understanding how to use optical tweezers with traditional linear momentum and then trapping and manipulating a particle with this kind of momentum. The experiment then advanced to testing the SLM to produce photons with orbital angular momentum and measuring the intensity of light after passing through many different holograms to find the best one for the experiment. Finally, the third phase involved adding the SLM to the previous optical tweezers set-up and trapping a micro-particle with OAM photons.

3.1 Achieving Linear Momentum Trapping

As laser beams naturally carry linear momentum, the set-up for achieving trapping with this kind of beam was the simpler of the two particle trapping set-ups. For this experiment a green 532 nm laser was used. This was set up on the left side of the optics bench and set to shine into the aperture of the optical tweezers. As the aperture needed to be saturated with light, however, two more pieces of equipment were added between the laser and the optical tweezers. The first item

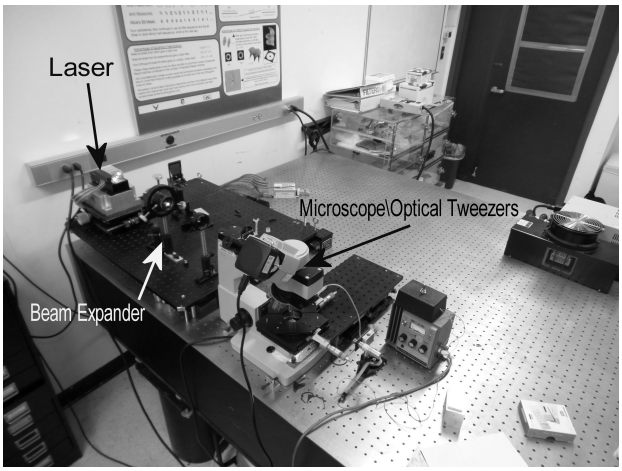

Figure 3.1: The set-up used for the linear momentum particle trapping phase of the experiment

added was a beam expander of variable magnification. For this experiment, it was set to 10x magnification. With this added, the laser beam was able to fill the whole aperture of the optical tweezers. An aperture was then added after the beam expander to cut off any light not needed to fill the aperture.

Once the beam was correctly positioned to shine straight through the aperture and down to the sample tray of the optical tweezers, a sample of particles was prepared on a glass slide and placed on the tray. For this experiment, the sample consisted of particles of polystyrene diluted with water. These particles were chosen due to their ease of acquisition and the fact that they are partially transparent to light. Different samples of these particles were made, some being more diluted or concentrated than others. The experiment also made use of three different sizes of particles: 0.5 micrometers, 1 micrometer, and 2 micrometers.

In order to record the motion of the particles under the influence of the beam, one of the eyepieces on the optical tweezers was replaced by a 1024 $\times$ 770 pixel resolution video camera that was connected to a computer. The computer had video recording software capable of making .wmv files that would be necessary for the later data analysis. With the sample set up and the camera and optical tweezers focused and ready to record, attention would turn to the computer, where

a preview of the recording would show a magnified version of the particles under the focus of the tweezers. If there were no particles in view, the tray the sample was sitting on would be manipulated using the knobs on the sides of the tray.

The next step was determining when to start the recording. As the purpose of the experiment was to measure the trapping force of the laser and thereby measure the momentum change the light imparts to the particle, it was important to not start the recording when the particle was already trapped. Because of this, it was necessary to start recording before the trapping occurred and then wait for the random Brownian motion of the particle to bring it near the trap. Once the particle actually was trapped, the recording stopped and the video file was transferred to the data analysis computer.

The analysis computer had a couple of different programs on it that were needed to complete the data analysis. The first program was the VeryDOC Video to GIF Converter. The purpose of this program is to take the previously recorded video and convert it into a sequence of images frame by frame. These images would then be loaded into the Able Particle Tracker, a program that can detect a particle in an image and then track its position through the following sequence of images. Once finished tracking the particle, the program would then produce a notepad document with a list of the x and y coordinates of the particle in pixels in every frame. This data would then be copied over to an Excel document where it could be manipulated freely.

Within the Excel sheet, various formulas were to convert the x and y coordinates to a radius. The radius was converted to micrometers from pixels using a previously determined conversion factor of $13.5\, pixels/\mu m$. This conversion factor was calculated using calibration tools included with the microscope. The velocity of the particle was determined using the traditional $v = \Delta r/\Delta t$ formula with the change in radius coming from the collected data and the change in time coming

from the amount of frames per second within the video. The exact frame at which the particle was trapped was then determined based on when the particle experienced the greatest velocity. A few frames before and after this frame would be taken and then the average velocity of these frames would be calculated.

After finding the average velocity of the trap, another equation has to be used to find the force of the light on the particle that is also experiencing Brownian motion. This equation is the Langevin equation,

$$m\ddot{\vec{r}} = -\gamma\dot{\vec{r}} + \vec{F}(\vec{r}) + \sigma\xi(t) \tag{3.1}$$

where m is the mass of the system determined from the density equation with the density of polystyrene being $1.05g/cm^3$, $\ddot{\vec{r}}$ and $\dot{\vec{r}}$ are the acceleration and velocity of the particle, respectively, γ is the scalar friction constant, $\vec{F}(\vec{r})$ is the total force on the particle, σ is the amplitude of the fluctuating force, and $\xi(t)$ is the equation governing the fluctuations of the random force [13]. The γ term can be found using the equation $\gamma = 6\pi\eta a$, where η is the viscosity of the liquid, in this case water, and a is the radius of the particle. The $\sigma\xi(t)$ is found using experimental data.

For this particular experiment, early data showed that $|\gamma\dot{\vec{r}}| \gg |m\ddot{\vec{r}}|$, allowing equation 3.1 to be rewritten as

$$\gamma\dot{\vec{r}} = \vec{F}(\vec{r}) + \sigma\xi(t). \tag{3.2}$$

Now the equation can be solved for the force by subtracting the experimentally determined $\sigma\xi(t)$, (found by recording the motion of a particle without a beam of light acting on it and finding the average force from many of such recordings) from the $\gamma\dot{\vec{r}}$ term. Finally, with this force found, the change in momentum imparted to

the particle by the light is found through the simple relation of $\vec{F} \times \Delta t = \Delta \vec{p}$.

3.2 Verifying the Laguerre-Gaussian Phase Shift

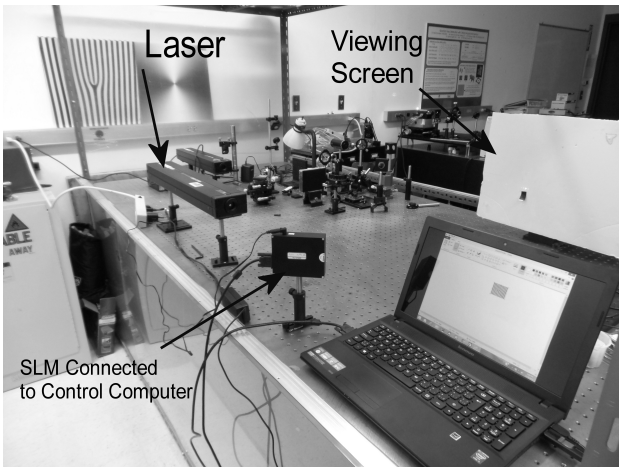

Figure 3.2: The set-up used to calibrate the SLM.

Before going through the process of adding the SLM to the previous set-up, it was important to determine that the SLM was working properly and was able to produce the necessary phase shift. To do this, an entirely different set up was built on the second optics bench in the lab. In this set up, a lower powered 543 nm laser was set up on the left side of the bench. The SLM was then set up in the path of the laser to reflect the light at a 90° angle so that the beam would hit a piece of cardboard set up for easy viewing of the beam.

After checking to make sure the beam was hitting the LCD part of the SLM, the computer hooked up to the SLM was turned on and a hologram was projected onto the LCD. The hologram needed to achieve the Laguerre-Gaussian phase shift was moved around in the paint program, corresponding to it being moved around on the SLM, until it was positioned just right for the beam to be passing through it. The correct position could be determined by examining the light after it was

reflected off the SLM and projected onto the cardboard. Once the first-order diffracted maxima had a doughnut shape with the hole exactly in the middle, the hologram was positioned correctly.

It was at this time that the hologram to be used in the final part of the experiment was chosen. The first decision was to use either a binary or blazed diffraction grating. Binary gratings feature a sharp transition between the black and white portions of the grating and produce a diffraction pattern that has equal intensities of light on both sides of the central diffraction maximum. Binary gratings have more smooth transitions from white to black through the use of various shades of gray. These gratings have diffraction patterns where the intensity of the light on one of the sides of the maximum is greater than the other side.

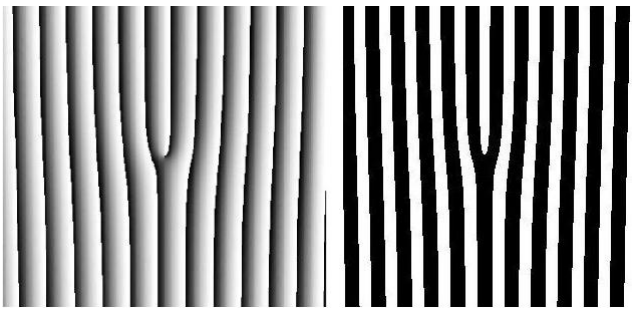

Figure 3.3: The two types of gratings tested in this experiment. On the left is a blazed grating and on the right is a binary. Both of these gratings correspond to the OAM quantum number value of $\ell = 1$.

Different settings for the code that generated the grating were also tested to find the values that gave the greatest intensity and best shape for the diffraction pattern. The number of lines within the forked part of the grating was one of these with higher values giving lower intensities but better shapes with more defined holes. Other parameters included the total size of the hologram (with smaller sizes giving greater space between maxima) and width of the black lines compared to the white lines (with more white giving greater intensity but a less defined diffraction pattern). With all these parameters in mind, the best hologram was

chosen and the SLM was moved to the previous set up for the final phase of the project.

3.3 Achieving OAM Trapping

For the final phase of the experiment, the experimental set-up was nearly identical to the first phase. The biggest change was that the SLM had to be added to the set-up, which meant that the laser had to be re-positioned so that when the light was reflected off the screen of the SLM, it would pass through into the microscope. A second aperture was also added to the set-up after the SLM and before the beam expander. This was used to make sure only the light from one of the rings of the diffraction pattern entered the microscope.

The data collection and analysis segment was also nearly identical to what occurred with linear momentum. The video was recorded and analyzed in the same way and all the previously used formulas were applied again to determine the force and momentum transferred to the particle. The force actually calculated, however, was different from the first experiment. While the linear momentum test was focused on the trapping force, this test focused on the force that was causing the particle to spin. As such, the video was not started until a particle was actually trapped so that only the orbiting force was calculated. With this force, the orbital momentum could then be calculated. An additional calculation was performed this phase in order to find the torque on the particle through the formula $\vec{\tau} = \vec{r} \times \vec{F}$.

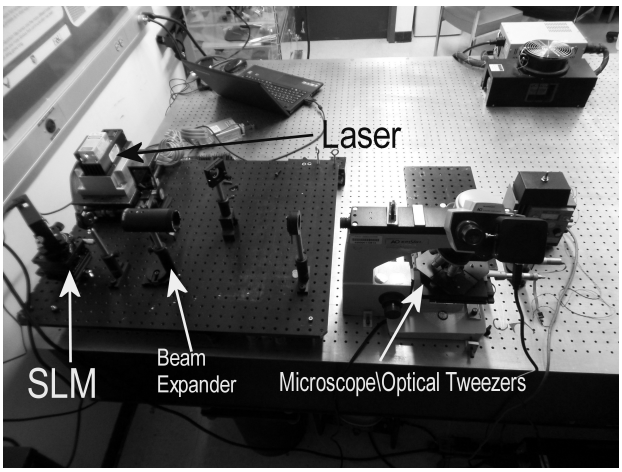

Figure 3.4: The set-up used for the OAM particle trapping phase of the experiment.

Chapter 4

Results

As the data for this thesis included over forty videos and excel documents, not all of the data has been included. Only certain key graphs and data points as well as some averages needed to explain the results can be found in the appendices. The full results of this experiment can be reviewed on the computer in the optics lab on the Boca Raton campus of FAU.

With regards to the first phase of the project, the goal was consistently met with polystyrene particles of size 1 and $2\mu m$. It was discovered early on that the camera did not have high enough resolution for the subsequent programs to analyze the $0.5\mu m$ particles. As such, all subsequent tests were done with the larger particle sizes.

Around ten tests were done for each size of particle. Once all of the videos were analyzed, the exact moment of trapping was found in each video's corresponding excel document. From each test, the data from the trap and a few frames before and after the trap were taken and added to an average document. From here, the average force for all tests for each particle was found. The graphs of these average documents are included in Appendix A. For the $1\mu m$ particle, the average force of the trap was found to be $2.30 \times 10^{-13} N$ and for the $2\mu m$ particle it was found to be $1.86 \times 10^{-13} N$. After subtracting out the Brownian motion force, which had

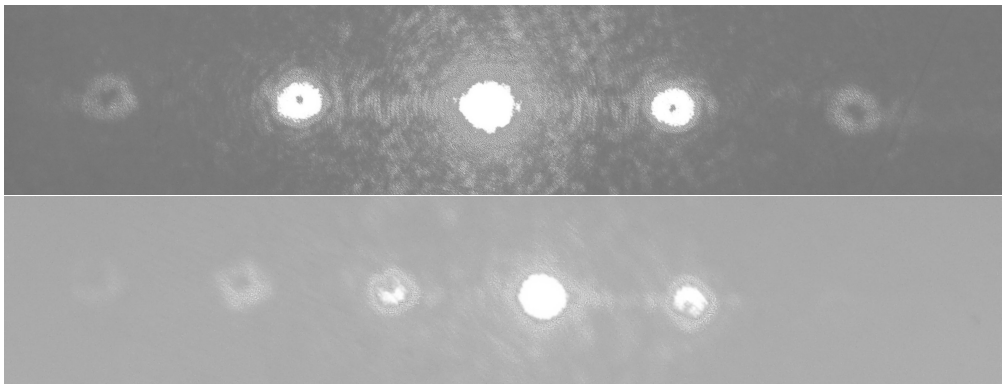

Figure 4.1: The top image is the diffraction pattern produced by a binary grating while the bottom is the pattern produced by a blazed grating.

a value of $3.27 \times 10^{-14}N$ for the $1\mu m$ particles and $7.02 \times 10^{-14}N$ for the $2\mu m$ particles, the two forces were calculated to be $1.97 \times 10^{-13}N$ and $1.15 \times 10^{-13}N$, respectively. As can be seen from the graph for this test in Appendix A, there was a definite trapping force which confined the particle to a certain location.

Moving onto the SLM calibration phase of the experiment, the choice of grating between binary and blazed was determined by the intensity of the diffraction pattern each one produced. It was initially believed that the blazed grating would produce a higher intensity due to the fact that the grating was designed to concentrate all the light from one side of the pattern into a single point.

Actual tests showed, however, that the binary grating gave an intensity of $223.0mW/m^2$ on one side of the diffraction maximum and $232.5mW/m^2$ on the other. In contrast, the blazed grating gave an intensity of $50.9mW/m^2$ and $82.8mW/m^2$ on the respective sides. While the blazed grating gave a much greater difference in intensities between sides, it cut down on the intensity of the whole system by a large amount. It was determined that this was due to the fact that the light had to pass through so much more of semi-transparent grey on the blazed compared to the binary grating where the totally transparent white bands were much larger.

With the binary grating chosen, determining the best value for ℓ was next.

After examining a couple of different gratings with different values of ℓ, it was decided that the $\ell = 1$ grating was the most effective. This is because although higher values of ℓ gave more distinct doughnut holes in the ring patterns, the holes started to become more elliptical with those higher values. The intensity of the light was also highest for this value. As such, the grating used for the final phase of the experiment was an $\ell = 1$ binary one.

The OAM experimental phase involved over forty different recordings. Unfortunately, the $2\mu m$ particles were too big to be caught by the force of the trap so all tests were done with the $1\mu m$ particles. Another major obstacle was that none of the videos showed evidence of any kind of circular motion on the particle's behalf. This was further confirmed by the data analysis that showed, for the most part, that the particle was not restricted from the center of the trap. There were a few tests that showed an empty center that the particle was restricted from accessing and their graphs and some data points are included in Appendix B, but these were far from the norm. For the particles that did show some semblance of circular motion, the average trapping force was found to be $1.25 \times 10^{-14} N$ and the torque imparted on them was $6.18 \times 10^{-21} Nm$.

Chapter 5

Conclusion

Referring back to the main goals of the experiment, success was achieved with all but one of them. A photon carrying linear momentum was shown to exert a trapping force on the order of 10 to 100 femto-Newtons. While this force definitely seems small, it is important to remember that particles that are experiencing the force are also very small. Trapping particles with linear momentum, therefore, is viable and, due to the sheer number of tests that were successful, is easy to achieve with the right equipment.

Similarly, creating the right types of laser beams for the different momenta was also consistently done. Producing Gaussian laser beams is very simple due to the fact that most laser beams are naturally Gaussian. With the help of the SLM, creating Laguerre-Gaussian beams also becomes easier. Not having to constantly switch slides of different gratings in a set-up to change one small parameter speeds up the process a great deal.

As for the OAM particle trapping goal, as stated before there was no sense of the particle experiencing circular motion, neither from the video nor from the data. After doing some further research and tests, it was speculated that this was due to two reasons. The first is that the particles used were too large to feel a force from the trap. A smaller particle would not need as great a force to move it

around, so making use of smaller particles would be greatly beneficial. As stated before, however, the video camera used for this experiment did not have a high enough resolution to distinguish particles smaller than $1\mu m$. This means that any future experiments will have to utilize a higher resolution camera. Unfortunately, for this experiment, there was neither the time nor the funding to find such a camera.

The other reason that might explain why the OAM trapping was not a success is that the laser used did not have a high enough intensity. It is easy to see that a higher intensity will lead to better trapping as a higher intensity means more photons, and the more photons entering a particle, the greater the force exerted on it. Through some tests on the intensity on the beam after it entered the microscope, it was discovered that the intensity was a mere $1.26W/m^2$. Compared to the intensity of the beam for the linear momentum trapping which had a value of $36.64W/m^2$, it is clear that the intensity was just too low for trapping to occur. It was discovered that this loss in intensity was due mostly to the addition of the SLM so there was no way around it. As such, any further tests will also need a higher intensity laser. Again, acquiring such a laser was not feasible for this experiment due to the time and funding constraints.

Appendices

Appendix A

Linear Momentum Data

The following is the data for the linear momentum tests on $1\mu m$ and $2\mu m$ particles. The data shown is an accumulation of samples taken from five different tests performed on each particle size. The sampling focused on a few points before, during, and after the trapping occurred for each test. The graphs show that for both sizes of particles, very far from the trap, the particles experience random forces, which is attributed to Brownian motion. As the particle gets closer to the trap, it experiences an increase in force from the light trap, pulling it into the trap. Once the particle is in the trap, the force becomes nearly zero with some amount of experimental error.

A.1 One Micrometer Particle

Radius (m)	Force (N)
2.13E-8	7.36E-15
3.11E-8	1.10E-14
4.70E-8	-2.60E-14
6.99E-8	3.77E-14

9.10E-8	8.28E-14
1.16E-7	-2.20E-14
1.31E-7	3.38E-14
1.43E-7	1.55E-14
1.67E-7	-2.78E-14
1.74E-7	-2.98E-14
2.36E-7	3.73E-14
2.37E-7	7.01E-15
2.43E-7	1.47E-14
2.57E-7	3.36E-14
3.12E-7	7.88E-14
5.60E-7	7.21E-14
8.32E-7	2.18E-13
8.42E-7	3.13E-13
8.53E-7	2.54E-13
1.14E-6	2.13E-13
1.41E-6	2.08E-13
1.42E-6	4.63E-13
1.59E-6	2.77E-13
1.60E-6	2.91E-13
1.92E-6	2.23E-13
1.96E-6	1.97E-13
1.97E-6	1.30E-13
1.99E-6	1.32E-13
1.99E-6	2.49E-14
2.13E-6	1.39E-13

2.21E-6	6.77E-14
2.35E-6	1.18E-13
2.37E-6	3.32E-14
2.41E-6	4.72E-15
2.50E-6	1.95E-13
2.52E-6	3.12E-14

Table A.1: One Micrometer Linear Momentum Data

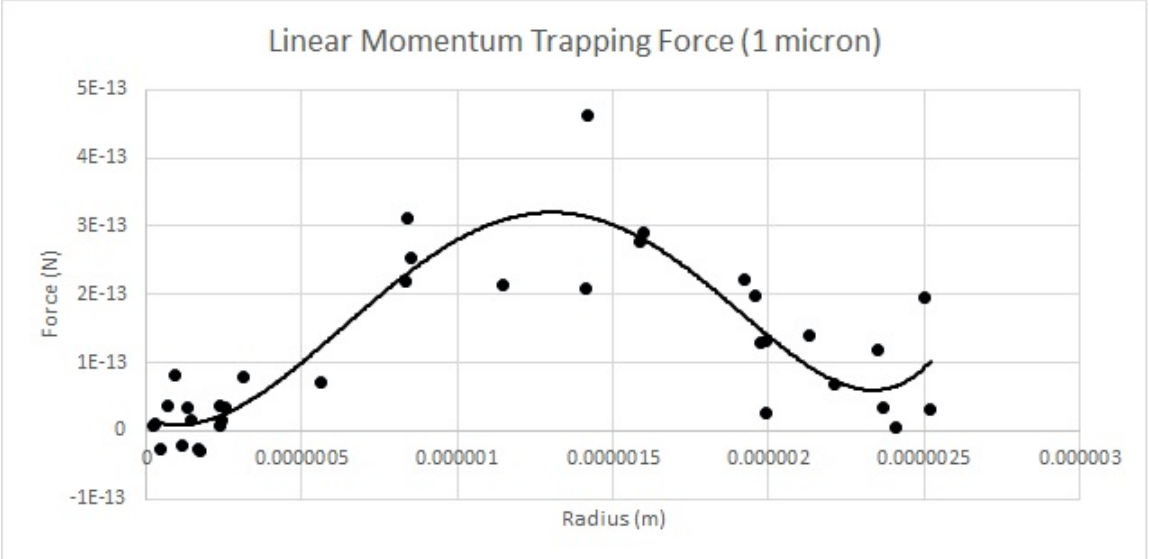

Figure A.1: One Micrometer Particle Linear Momentum Trapping Force

A.2 Two Micrometer Particle

Radius (m)	Force (N)
6.40E-9	-6.98E-14
1.08E-8	-1.38E-14
2.52E-8	-5.83E-14

3.55E-8	-5.80E-14
5.36E-8	-4.81E-14
8.65E-8	-4.87E-14
1.08E-7	-6.36E-14
1.16E-7	-2.61E-14
1.21E-7	-2.97E-14
1.24E-7	-6.77E-14
1.25E-7	-5.42E-14
1.38E-7	-6.45E-14
1.71E-7	-5.65E-14
1.76E-7	-6.79E-14
1.84E-7	-6.72E-14
2.15E-7	-5.71E-14
2.21E-7	-2.59E-14
6.92E-7	1.76E-13
7.01E-7	1.74E-13
9.73E-7	2.47E-13
1.29E-6	3.13E-13
1.40E-6	2.28E-13
1.61E-6	3.13E-13
1.84E-6	7.59E-14
1.95E-6	7.16E-14
2.18E-6	2.00E-13
2.25E-6	5.87E-14
2.34E-6	-3.39E-14
2.36E-6	-6.05E-14

2.50E-6	-6.80E-14
2.51E-6	3.51E-14
2.66E-6	-3.33E-15
2.85E-6	6.63E-15
2.94E-6	-3.26E-14

Table A.2: One Micrometer Linear Momentum Data

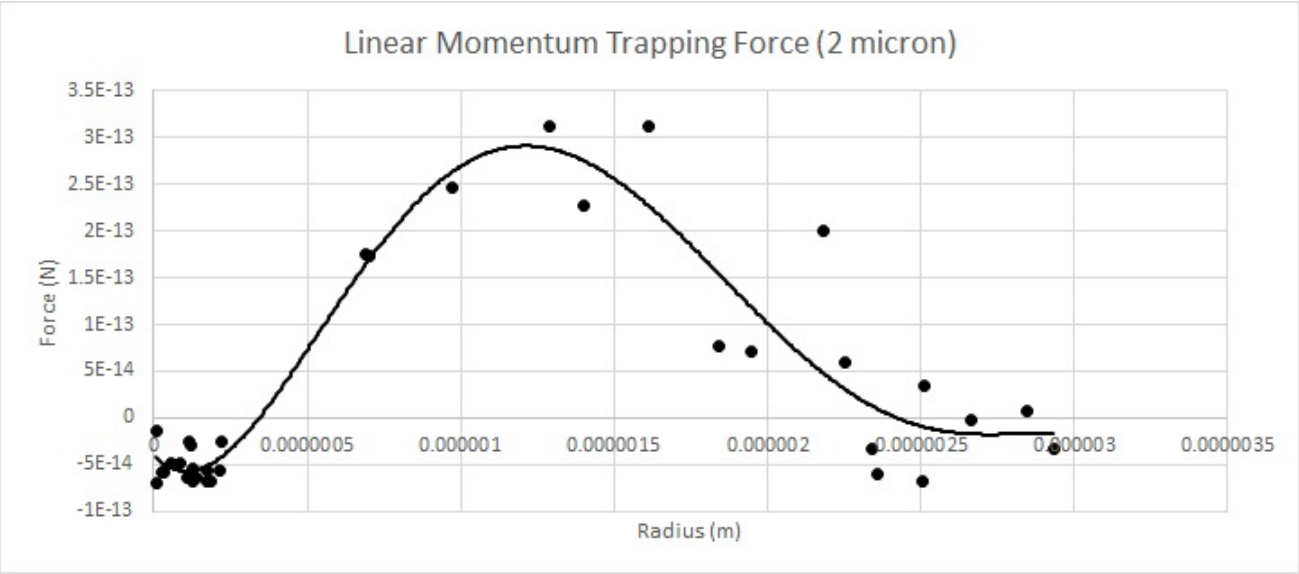

Figure A.2: Two Micrometer Particle Linear Momentum Trapping Force

Appendix B

OAM Data

The following is a sampling of data taken from the tests done with orbital-angular momentum. As stated earlier, the complete data is too large to be included in this thesis. The tables are just segments of the excel data sheets. The graphs, however, show the full range of data. The data has been collected from two out of the total four successful tests in the whole experiment. The first table and set of graphs is for the fourth test performed and the second table and set of graphs is for the ninth test performed. The first graph shows the position of the particle in an $x-y$ plane in all frames recorded and the second graph shows the force on the particle at a certain radius away from the trap. The position graphs show that the particle is restricted from entering some circle of a certain radius, hinting at some kind of circular motion. The force graphs show that the particle does not experience a force too close or too far away from the trap, suggesting the particle is being held in a radius range.

B.1 Fourth OAM Test

Time (s)	X(m)	Y(m)	Radius (m)	Force (N)

...	...	...	...	...
2	-6.75E-8	-6.50E-8	9.37E-8	4.93E-16
2.02	7.74E-8	-5.06E-8	9.25E-8	0
2.04	7.74E-8	-5.06E-8	9.25E-8	2.44E-14
2.06	6.81E-8	-1.34E-7	1.51E-7	2.57E-15
2.08	5.29E-8	-1.47E-7	1.57E-7	0
2.1	5.29E-8	-1.47E-7	1.57E-7	3.91E-14
2.12	1.23E-7	-2.17E-7	2.49E-7	5.52E-14
2.14	8.54E-8	-8.19E-8	1.18E-7	1.91E-14
2.16	1.19E-7	-1.12E-7	1.64E-7	0
2.18	1.19E-7	-1.12E-7	1.64E-7	4.06E-14
2.2	1.49E-7	-2.13E-7	2.60E-7	7.67E-14
2.22	5.68E-8	5.32E-8	7.78E-8	6.53E-14
2.24	1.37E-7	-1.88E-7	2.33E-7	0
2.26	1.37E-7	-1.88E-7	2.33E-7	6.01E-14
2.28	5.34E-8	7.26E-8	9.02E-8	7.52E-15
2.3	9.27E-8	5.54E-8	1.08E-7	0
2.32	9.27E-8	5.54E-8	1.08E-7	4.81E-14
2.34	1.65E-7	-1.49E-7	2.22E-7	7.48E-14
2.36	9.08E-8	-3.89E-7	4.00E-7	2.69E-14
2.38	1.56E-8	-3.36E-7	3.36E-7	0
2.4	1.56E-8	-3.36E-7	3.36E-7	7.67E-15
2.42	2.38E-8	-3.53E-7	3.54E-7	4.73E-15
2.44	-1.12E-7	-3.48E-7	3.66E-7	0
2.46	-1.12E-7	-3.48E-7	3.66E-7	3.67E-14
2.48	1.63E-7	-2.25E-7	2.78E-7	4.89E-14

2.5	9.54E-8	-1.31E-7	1.62E-7	3.66E-14
2.52	4.03E-8	6.37E-8	7.54E-8	0
2.54	4.03E-8	6.37E-8	7.54E-8	4.99E-15
2.56	7.28E-8	4.81E-8	8.72E-8	4.24E-14
2.58	1.87E-7	1.30E-8	1.88E-7	0
2.6	1.87E-7	1.30E-8	1.88E-7	3.68E-14
2.62	7.59E-8	6.61E-8	1.01E-7	4.51E-15
2.64	7.48E-8	8.24E-8	1.11E-7	7.93E-15
2.66	7.29E-8	5.70E-8	9.25E-8	0
2.68	7.29E-8	5.70E-8	9.25E-8	9.83E-15
2.7	3.66E-9	-6.91E-8	6.92E-8	1.50E-14
2.72	3.51E-8	-9.86E-8	1.05E-7	1.09E-13
2.74	3.21E-7	1.72E-7	3.64E-7	0
2.76	3.21E-7	1.72E-7	3.64E-7	1.088E-13
...	...	...	...	...

Table B.1: Fourth OAM Test

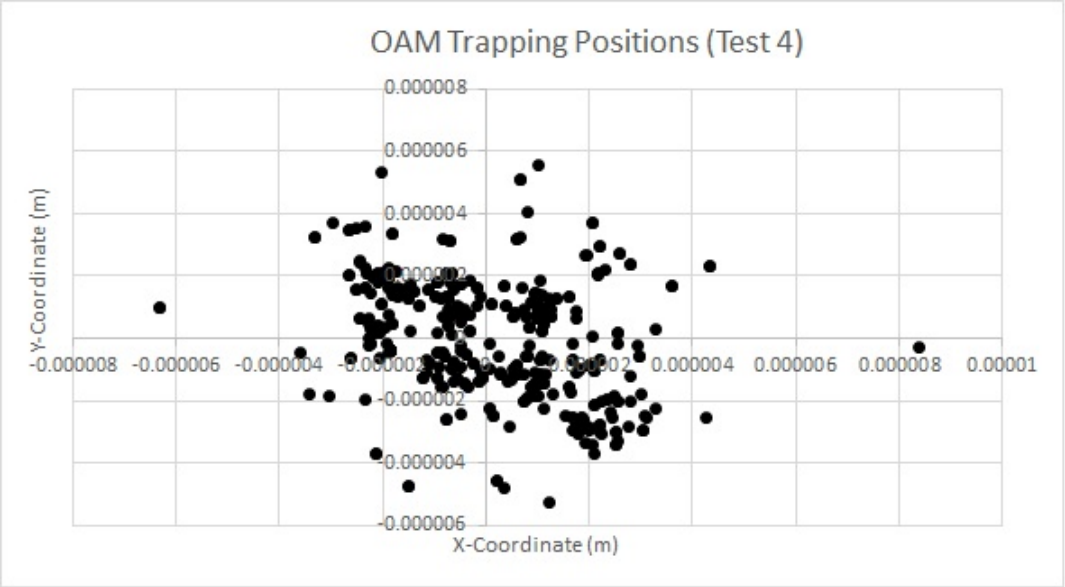

Figure B.1: Fourth OAM Test Trapping Positions

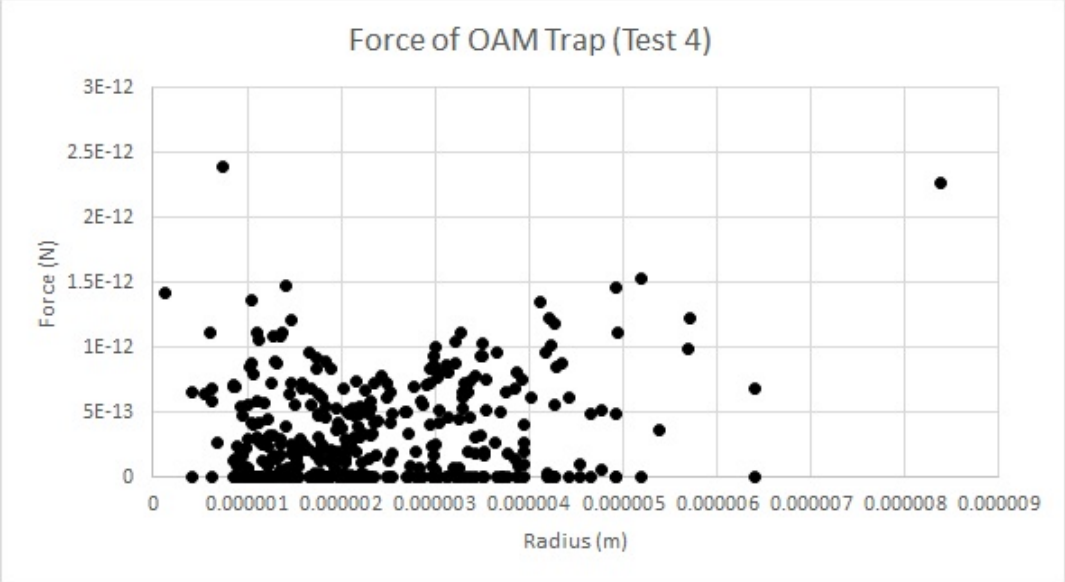

Figure B.2: Fourth OAM Test Trapping Force

B.2 Ninth OAM Test

Time (s)	X(m)	Y(m)	Radius (m)	Force (N)
...	...	...	...	...
2.00	1.44E-7	4.22E-8	1.50E-7	1.92E-14
2.02	-1.18E-7	-3.74E-9	1.18E-7	3.21E-14
2.04	-1.16E-7	-1.27E-8	1.16E-7	2.75E-14
2.06	-1.91E-8	-1.03E-7	1.04E-7	2.69E-14
2.08	-1.18E-7	-3.74E-9	1.18E-7	2.45E-14
2.10	-1.37E-7	-3.74E-9	1.37E-7	2.33E-14
2.12	-1.18E-7	2.43E-7	2.70E-7	3.66E-14
2.14	-1.06E-7	-5.83E-9	1.06E-7	2.75E-14
2.16	-1.18E-7	-3.74E-9	1.18E-7	3.27E-14
2.18	-1.18E-7	-3.74E-9	1.18E-7	2.37E-14
2.20	-2.28E-7	1.06E-7	2.52E-7	2.07E-14
2.22	-2.22E-7	-2.65E-8	2.23E-7	2.17E-14
2.24	-1.97E-7	-1.36E-8	1.97E-7	2.30E-14
2.26	-2.04E-7	8.27E-8	2.20E-7	3.04E-14
2.28	-1.94E-7	1.15E-7	2.26E-7	2.07E-14
2.30	-1.97E-7	-1.36E-8	1.97E-7	2.39E-14
2.32	-3.15E-7	-1.03E-7	3.32E-7	3.29E-14
2.34	1.73E-7	3.23E-8	1.76E-7	8.25E-15
2.36	-1.18E-7	-3.74E-9	1.18E-7	3.27E-14
2.38	-1.18E-7	-3.74E-9	1.18E-7	1.39E-14
2.40	1.59E-7	3.22E-8	1.63E-7	1.27E-14
2.42	-1.18E-7	2.43E-7	2.70E-7	3.22E-14
2.44	2.53E-7	9.16E-8	2.69E-7	9.43E-16

2.46	1.88E-7	1.99E-8	1.89E-7	2.66E-15
2.48	-1.18E-7	-3.74E-9	1.18E-7	4.11E-16
2.5	-1.60E-7	-1.13E-7	1.96E-7	2.76E-14
2.52	-1.45E-7	-1.14E-7	1.85E-7	2.76E-14
2.54	-1.60E-7	-1.13E-7	1.96E-7	3.27E-14
2.56	-1.60E-7	-1.13E-7	1.96E-7	3.27E-14
2.58	-1.60E-7	-1.13E-7	1.96E-7	3.27E-14
2.60	-1.60E-7	-1.13E-7	1.96E-7	4.25E-15
2.62	-1.08E-7	-1.24E-8	1.09E-7	2.88E-14
2.64	-1.18E-7	-3.74E-9	1.18E-7	3.07E-14
2.66	-1.13E-7	-7.94E-9	1.13E-7	2.77E-15
2.68	-1.97E-7	-1.36E-8	1.97E-7	1.34E-13
2.70	-5.78E-7	-1.36E-7	5.94E-7	5.12E-14
2.72	-3.40E-7	-2.01E-7	3.95E-7	5.18E-14
2.74	-1.91E-8	1.94E-7	1.95E-7	3.29E-16
2.76	-1.18E-7	-3.74E-9	1.18E-7	3.29E-16
...	...	...	...	...

Table B.2: Ninth OAM Test

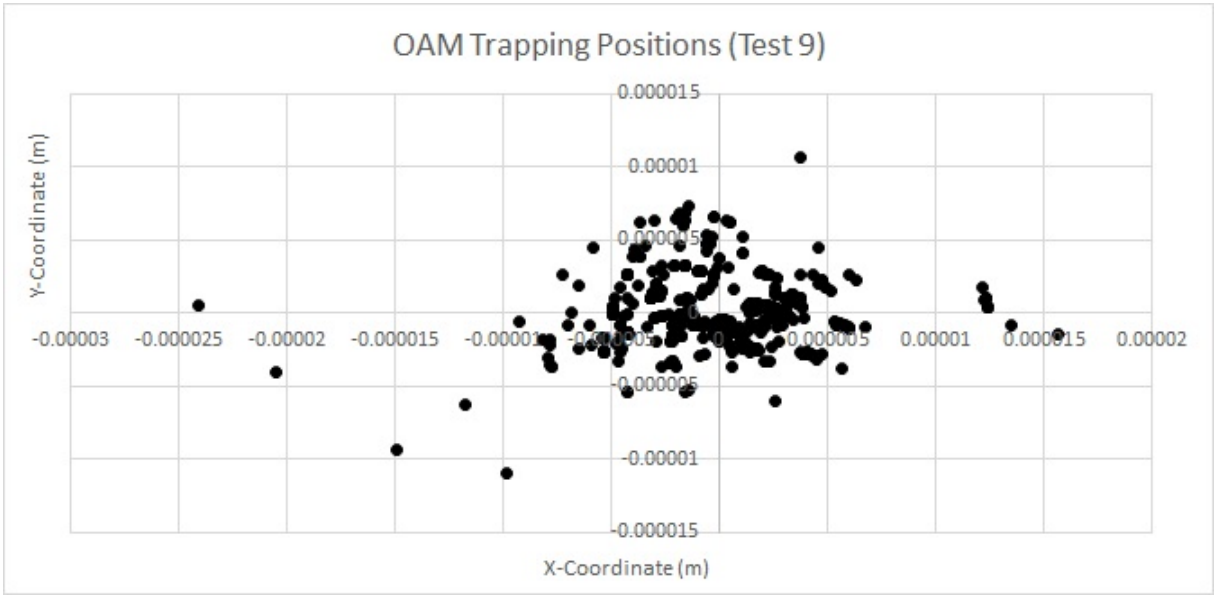

Figure B.3: Ninth OAM Test Trapping Positions

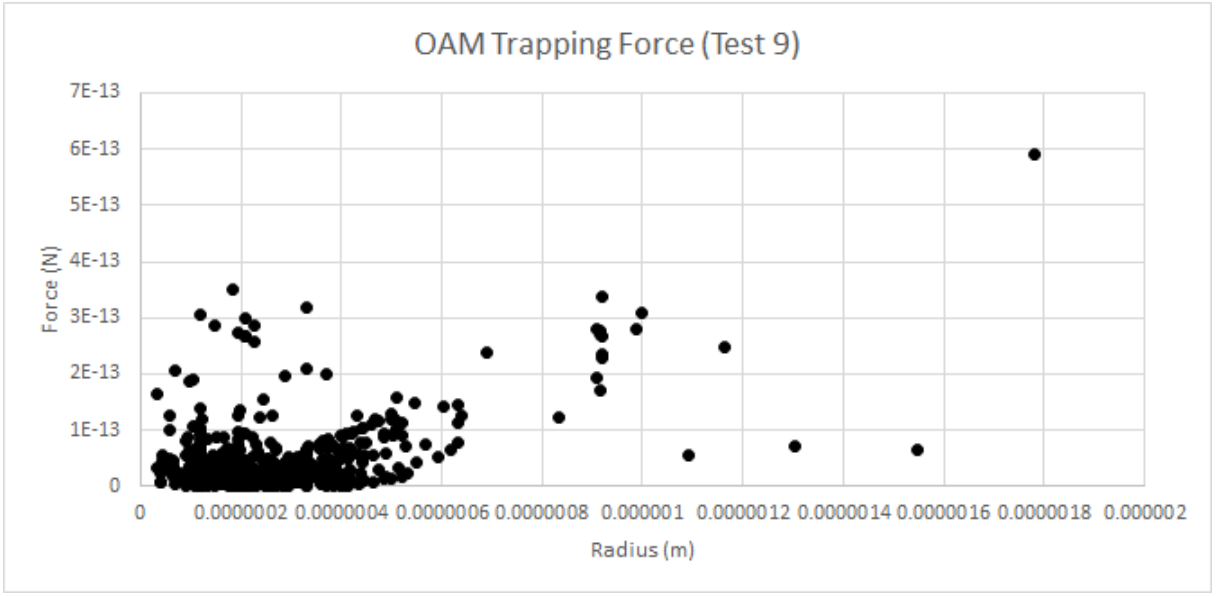

Figure B.4: Ninth OAM Test Trapping Force

Appendix C

Code

C.1 Binary Generating Code

The following is the Matlab code used to generate the $\ell = 1$ binary grating seen earlier in the text. For the original, unaltered code, please see [5].

```
clear
R=1;              % radius of curvature of wavefront
A=1;              % oblique incidence (1=oblique 0=collinear): straight fringes
B=0;              % expanding (1=yes 0=no): concentric fringes
L=1;             % topological charge
Lambda=0.5;         % fringe spacing
aspect=0.5;       % fraction of fringe period that is white/clear
res=500;         % resolution (res x res number data pts calculated)
range=5;         % range (plotted in x in y on interval [-range,range]

param(:,1)=-range:2.0001*range/res:range;      % list of x values
param(:,2)=range:-2.0001*range/res:-range;     % list of y values

for x=1:res
    for y=1:res
        % wave interference function
        psi(x,y)=L*atan(param(y,2)/param(x,1))-2*pi*param(x,1)/Lambda*A+ ...
        ((param(x,1))^2+(param(y,2))^2)/R^2*B+pi/2;

        % transmittance function (the one plotted)
        T(x,y)=(1+(cos(psi(x,y)+pi*(1+param(x,1)/abs(param(x,1))))*1/2) -...
        cos(aspect*pi)*L)/abs(cos(psi(x,y)+pi*(1+param(x,1)/...
```

```
        abs(param(x,1)))*1/2)-cos(aspect*pi)*L)*1/2;
    end
end

contourf(T)     % filled contour plot
colormap gray;
axis off;
```

C.2 Blazed Generating Code

The following is the Matlab code used to generate the $\ell = 1$ blazed grating seen earlier in the paper. Again, the code provided is the code with the exact parameters used in this experiment. The original code can be found at [6].

```
clear all;
n = 2^10; % Size of the array
mask = zeros(n); % Sets the mask as an array of all zeros initially
I = 1:n; % Setup size of array
x = I-n/2;
y = n/2-I;
[X,Y] = meshgrid(x,y); % Initiate cartesian coordinates
theta = atan2(Y,X); % Transforming to polar coordinates
r = sqrt(X.^2 + Y.^2); %
D = 3*pi;
K = 0.11.*2*pi/D; % Grating Constant
L = 1; % Sets the value of L
% This is where the magic happens. A is the grating function
A = (((L.*theta)./1) - K.*X);
% This gives the mask the blazed appearance due to the modulo function
%mask = (1/sqrt(2)).*exp(-1i.*0.11*mod(A,2*pi));
mask = exp(-1i.*0.3*mod(A,2*pi));
figure
imagesc(real(mask))
colormap(gray)
axis off
```

Appendix D

References

[1] Okun, L. B. Photon: History, Mass, Charge. Acta Phys.Polon. 2006: B37: 565-574. doi:arXiv:hep-ph/0602036.

[2] Compton, A. H. A Quantum Theory of the Scattering of X-Rays by Light Elements. Phys. Rev. 1923: 21(5): 483-502. doi:10.1103/PhysRev.21.483.

[3] Bowman, R. & Padgett, M. Tweezers with a Twist. Nat. Photonics. 2011: 5(6): 343-348. doi:dx.doi.org/10.1038/nphoton.2011.81.

[4] Padgett, M., Courtial, J., & Allen, L. Light's Orbital Angular Momentum. Phys. Today. 2004: 57(5): 35-40. doi:10.1063/1.1768672

[5] Jain, A. Journal [Internet]. Stony Brook: Stony Brook University; 2005 [cited 2015 April 25]: http://laser.physics.sunysb.edu/ amol/journal/journal.xml.

[6] Sztul, H. (2008). Optical vortices: Angular momentum of light, energy propagation, and imaging. [Ph. D. thesis on the Internet]. [New York]: City University of New York. [cited 2015 April 26]. Available from ProQuest Dissertations and Theses. Order No. 3325437

[7] Chapter 2: Gaussian Beam Propagation [Internet]. Tainan City, Taiwan: National Cheng Kung University; [Date Unknown] [cited 2015 April 26]. Available from: http://www.phys.ncku.edu.tw/ cctsai/teaching/10202/gaussian

[8] Ashkin, A. Acceleration and Trapping of Particles by Radiation Pressure. Phys. Rev. Lett. 1970: 24(4): 156-159. doi:10.1103/PhysRevLett.24.156.

[9] Zhang, H., & Liu, K.-K. Optical tweezers for single cells. J R Soc Interface. 2008: 5(24): 671–690. doi:10.1098/rsif.2008.0052

[10] Awschalom, D., Beletic, J., Bucksbaum, P., Ha, T., Heinz, T., Kath, W., ..., Sension, R. Executive Summary- Report of the Optics and Photons Subcommittee of the MPS Advisory Committee: Science Opportunities in Optics and Photonics. [no date] Retrieved from http://nsf.gov/mps/advisory/mpsac_other_reports/optics_and_photonics-final_from_subcommittee.pdf.

[11] Bozinovic, N., Yue, Y., Ren, Y., Tur, M., Kristensen, P., Huang, H., ..., Ramachandran, S. Terabit-Scale Orbital Angular Momentum Mode Division Multiplexing in Fibers. Science. 2013: 340(6140): 1545-1548. doi: 10.1126/science.1237861.

[12] Molloy, J. E. & Padgett, M. J. Lights, Action: Optical Tweezers. Contemp Phys. 2002: 43(4): 241-258. doi:10.1080/00107510110116051.

[13] Schulten, K. Chapter 4:Smoluchowski Diffusion Equation [Internet]. Chicago: University of Illinois Non-Equilibrium Statistical Mechanics; 1999 [cited 2015 April 25]. Available from: http://www.ks.uiuc.edu/Services/Class/PHYS498/LectureNotes/chp4.pdf.